Glycolipid-Containing Nanoparticle Vaccine Engages Invariant NKT Cells to Enhance Humoral Protection against Systemic Bacterial Infection but Abrogates T-Independent Vaccine Responses

Travis Shute,*[,1] Eyal Amiel,[†,1,2] Noran Alam,* Jennifer L. Yates,[†,3] Katya Mohrs,[†,4] Elizabeth Dudley,* Briana Salas,*[,5] Chloe Mesa,* Adriana Serrata,* Daniel Angel,[‡] Brandy K. Vincent,[‡] Amanda Weyers,[§] Paula A. Lanthier,[†] Emilie Vomhof-Dekrey,[†,6] Rachel Fromme,[¶] Mitchell Laughlin,[¶] Olivia Durham,[¶] Jianjun Miao,[§] Devon Shipp,[¶] Robert J. Linhardt,[§] Kelly Nash,[‡] and Elizabeth A. Leadbetter*

CD4$^+$ T cells enable the critical B cell humoral immune protection afforded by most effective vaccines. We and others have recently identified an alternative source of help for B cells in mice, invariant NK T (iNKT) cells. iNKT cells are innate glycolipid-specific T cells restricted to the nonpolymorphic Ag-presenting molecule CD1d. As such, iNKT cells respond to glycolipids equally well in all people, making them an appealing adjuvant for universal vaccines. We tested the potential for the iNKT glycolipid agonist, α-galactosylceramide (αGC), to serve as an adjuvant for a known human protective epitope by creating a nanoparticle that delivers αGC plus antigenic polysaccharides from *Streptococcus pneumoniae*. αGC-embedded nanoparticles activate murine iNKT cells and B cells in vitro and in vivo, facilitate significant dose sparing, and avoid iNKT anergy. Nanoparticles containing αGC plus *S. pneumoniae* polysaccharides elicits robust IgM and IgG in vivo and protect mice against lethal systemic *S. pneumoniae*. However, codelivery of αGC via nanoparticles actually eliminated Ab protection elicited by a T-independent *S. pneumoniae* vaccine. This is consistent with previous studies demonstrating iNKT cell help for B cells following acute activation, but negative regulation of B cells during chronic inflammation. αGC-containing nanoparticles represent a viable platform for broadly efficacious vaccines against deadly human pathogens, but their potential for eliminating B cells under certain conditions suggests further clarity on iNKT cell interactions with B cells is warranted. ***The Journal of Immunology*****, 2021, 206: 1806–1816.**

A successful vaccine is one that generates a strong humoral response and maintains long-lasting B cell memory. This has traditionally been achieved by engaging APC, B cell, and CD4 T cell cross-talk, but invariant NKT (iNKT) cells can also provide B cell coactivation (1, 2). iNKT cells acutely activated by the glycolipid α-galactosylceramide (αGC) enhance humoral B cell immune responses to coadministered proteins and polysaccharides (3–5). iNKT cells are unique in that they are restricted to the nonpolymorphic Ag-presenting molecule CD1d. As such, there will be no allelic variation in the response of iNKT cells to glycolipid activation in different individuals. This makes iNKT cells an ideal source of help for B cells in the context of a vaccine for large populations of humans with diverse haplotypes.

Previous attempts to harness αGC for vaccine development in humans and mice have found αGC to be well tolerated and safe but were complicated by the fact that high doses of soluble αGC-induced anergy in murine iNKT cells (6–9). Nanoparticles (nanoP) have recently been introduced as a novel means to tailor delivery of αGC. NanoP are characterized by their small size, which facilitates their uptake by APC through an endocytosis mechanism (10). APC such as macrophages usually take up large nanoP (500–5000 nm), whereas other APC such as dendritic cells usually take up smaller

*UT Health San Antonio, San Antonio, TX; [†]Trudeau Institute, Saranac Lake, NY; [‡]Department of Astronomy and Physics, The University of Texas at San Antonio, San Antonio, TX; [§]Rensselaer Polytechnic Institute, Troy, NY; and [¶]Center for Advanced Material Processing, Department of Chemistry and Biomolecular Science, Clarkson University, Potsdam, NY 13699

[1]T.S. and E.A. contributed equally.

[2]Current address: University of Vermont School of Medicine, Burlington, VT.

[3]Current address: Wadsworth Center, Albany, NY.

[4]Current address: Regeneron, Inc., Tarrytown, NY.

[5]Current address: Our Lady of the Lake, San Antonio, TX.

[6]Current address: University of North Dakota, Grand Forks, ND.

ORCIDs: 0000-0003-2169-2918 (T.S.); 0000-0002-1578-8705 (E.A.); 0000-0001-8841-9401 (J.L.Y.); 0000-0002-7709-7520 (B.S.); 0000-0003-2958-5973 (P.A.L.); 0000-0003-3818-5330 (E.V.-D.); 0000-0002-8709-1667 (D.S.).

Received for publication November 12, 2020. Accepted for publication February 17, 2021

This work was supported by Clarkson University/Trudeau Institute Partnership Grant CUTIP (to E.A.L. and D.S.), by National Institute of Allergy and Infectious Diseases, National Institutes of Health Grants R56 AI104788-01A1 and 5 R21 AI113517-03 to E.A.L., T32 AI138944 and TL1 TR002647 to T.S., and T32 AI049823 to E.A., J.L.Y., and E.V.-D., and by the Voelker Fund Young Investigator Award (to E.A.L.).

Address correspondence and reprint requests to Elizabeth A. Leadbetter, UT Health San Antonio, 7703 Floyd Curl Drive, San Antonio, TX 78229. E-mail address: leadbetter@uthscsa.edu

The online version of this article contains supplemental material.

Abbreviations used in this article: αGC, α-galactosylceramide; βGC, β-galactosylceramide; i.n., intranasally; iNKT, invariant NKT; iNKT$_{FH}$, iNKT follicular helper; LCMS, liquid chromatography/mass spectrometry; nanoP, nanoparticle; nanoP-αGC, nanoP containing αGC; nanoP-βGC, nanoP containing βGC; nanoP-αGC-SpPS, nanoP containing αGC and SpPS from SpPS3; nanoP-PBS, nanoP containing PBS; nanoP-SpPS, nanoP containing SpPS; PEG, polyethylene glycol; PLGA, poly(DL-lactic-coglycolic acid); SpPS, *S. pneumoniae* polysaccharide serotype; WT, wild-type.

www.jimmunol.org/cgi/doi//doi.org/10.4049/jimmunol.2001283

nanoP (200–500 nm) (11). NanoP size can also affect their distribution to lymphatic tissue. For example, small nanoP can pass through the extracellular matrix and move through lymphatic drainage before being engulfed by resident APC in secondary lymphoid organs (12). Larger nanoP, bigger than 100 nm, usually stay at the injection site until they are taken up by local APC for indirect delivery to lymphatic tissue (13). Both large 500–2000-nm and small 90-nm nanoP loaded with αGC have been reported to robustly stimulate iNKT cell proliferation in vitro and in vivo (14, 15). Because nanoP deliver their cargo very efficiently, this delivery mechanism enables 1000× dose sparing (16) and suggests a novel means to avoid the anergy induced by high concentrations of αGC (14, 17, 18).

NanoP are able to cross mucosal barriers, can be easily loaded with a variety of payloads, and have been Food and Drug Administration approved for more than 50 years. A broad range of nanoP platforms, including poly(DL-lactic-coglycolic acid) (PLGA), have been pursued as potential vaccine and therapeutic strategies against an array of clinically relevant diseases (reviewed in Ref. 19). PLGA delivery of Ag drives a stronger and more long-lasting Ab response when compared with soluble delivery (20). Previous formulations of PLGA nanoP for drug delivery to humans have alleviated negative charges of the particles through surface modification by PEGylation (21) or chitosan coating (22). PEGylation of the PLGA polymer also enables some shielding from recognition by the reticuloendothelial system, providing a so-called "stealth effect" from this circulatory clearance system. Polyethylene glycol (PEG) enhances internalization and postinternalization escape from lysosomes, which is used when cytosolic delivery of nanoP cargo is preferred. However, the addition of PEG to the outer surface of the nanoP has a few unfortunate consequences (23). For one, the PEG molecules can obscure targeting molecules attached to the outside of a nanoP, which then requires further modifications or tethering to overcome (24). Problematically, repeated immunization with PEGylated liposomes induces a robust IgM immune response in the spleen, followed by enhanced clearance, suggesting the PEG itself may be an immune target (25–27). Therefore, it will be advantageous to use a nanoP that is able to deliver adjuvant to the relevant Ag-specific B cells without requiring this additional component. Another pitfall of nanoP is a rapid burst of drug release at the time of administration. This mechanism of drug release is common for nanoP with drugs or Ags loaded on their surface and may be avoided by embedding the Ag within the entire nanoP.

We hypothesize that delivery of lower doses of αGC embedded in a highly efficient PLGA nanoP platform will avoid anergy and facilitate iNKT cell help for protective B cell humoral responses. *Streptococcus pneumoniae* is an ideal candidate for testing a vaccine platform comprised of nanoP delivery of iNKT-activating glycolipids because the protective epitopes have already been carefully defined and their protective potential confirmed. *S. pneumoniae* is an extracellular pathogen and the most common cause of pneumonia in humans. The successful peptide-conjugate vaccine currently in use in the clinic, Prevnar13, drives protective immune responses against 13 different serotype-specific polysaccharide epitopes in at risk populations and has dramatically reduced the number of yearly invasive pneumococcal cases (28). However, 500,000 children still die every year, with nonvaccine serotypes gaining in frequency (29–31), and 53% of the infant population worldwide still do not have access to these vaccines (VIEW-Hub, https://view-hub.org). Polysaccharides are known to be the target of protective IgM and IgG Abs, which are critical for survival against septic *S. pneumoniae* infections, as agammaglobulinemic and splenectomized patients have more severe disease (32–34). Conventional peptide specific T cells provide key helper signals to drive activation and class switch by polysaccharide-specific B cells in the context of the peptide-conjugate Prevnar13 vaccine (35). iNKT cells can be engaged to help generate similar humoral immunity against pneumococcal capsular polysaccharides (15), so *S. pneumoniae* provides a clinically relevant disease model to test the protective efficacy of this novel nanoP vaccine platform using codelivery of αGC adjuvant plus known protective epitopes in one particle or αGC nanoP in combination with current vaccines.

In this study, we show that PLGA nanoP simultaneously loaded with both αGC and *S. pneumoniae* polysaccharides can simultaneously activate iNKT cells and B cells in vitro and in vivo. As suspected, efficient PLGA delivery of αGC avoids iNKT anergy after multiple administrations. The cooperation induced by PLGA nanoP containing αGC (nanoP-αGC) and polysaccharide Ags induces both IgM and IgG humoral memory and provides protection against a lethal septic *S. pneumoniae* challenge. Intriguingly, we also find that glycolipid-containing nanoP do not amplify a submaximal humoral response induced by current T-dependent Ag containing vaccines and actually inhibit humoral responses induced by T-independent Ag containing vaccines. As such, these data suggest that acute activation of iNKT cells by codelivery of a glycolipid and protective antigenic epitopes is a viable vaccine strategy against numerous different infectious diseases but caution against codelivering αGC in combination with current *S. pneumoniae* vaccines. This is consistent with previous studies demonstrating αGC-induced development of iNKT follicular helper ($iNKT_{FH}$) cells, which provide help for B cells following acute activation (36, 37), compared with engagement of a killer phenotype, which negatively regulates B cells during chronic inflammation (38). However, more studies are required to dissect the specific mechanism of B cell activation elicited by codelivery of αGC and T-dependent Ag versus inhibition mediated during codelivery of αGC nanoP and T-independent Ag.

Materials and Methods

NanoP preparation and analysis

PLGA nanoP were prepared by laboratories of Dr. K. Nash (The University of Texas San Antonio, San Antonio, TX) or Dr. R. Lindhart (Rensselaer Polytechnic Institute, Albany, NY) via double emulsion. This included an aqueous phase of 0.5 mg/ml BSA in 8 mM trisodium citrate dehydrate (pH 8) with or without 0.8 mg/ml *S. pneumoniae* polysaccharide serotype (SpPS) 3 (American Type Culture Collection). The organic phase contained 50 mg/ml PLGA in dichloromethane. αGC-containing nanoP included an additional 12.5 μg/ml glycolipid, αGC (Chemistry Abstract Service no. 158021-47-7) or β-galactosylceramide (βGC) (Avanti Polar Lipids). BSA/SpPS3/citrate buffer solution was added dropwise to PLGA/αGC solution in dichloromethane (50 mg/ml). Sonication of this solution was done on ice (85% A at 100 W) for 10 s on/10 s off twice by Sonics and Materials Vibra-Cell sonicator with a 5/64-inch probe (provided by Dr. G. Zhong, UT Health San Antonio). This emulsion was transferred to 4 ml of 10% sucrose or 0.3% w/v Vitamin E TPGS followed by further sonication (85% A at 100 W) for 10 s on/10 s off three times before rotary evaporation (RotoVap), and washing with 1 ml 0.3% w/v Vitamin E TPGS to remove larger particles. NanoP size and glycolipid content were characterized by Zetasizer (Malvern) and liquid chromatography/mass spectrometry (LCMS) as described below.

LCMS

RPI. αGC and βGC were quantified by a liquid chromatography/tandem mass spectrometry method running in multiple reaction monitoring mode. Chromatographic separation was achieved using a Waters HPLC column (BEH C8, 3 × 50 mm). The mobile phases were A, 5 mM ammonium formate in water with 0.2% formic acid; and B, 5 mM ammonium formate in methanol with 0.2% formic acid. The gradient started from 85% B to 100% B in 5 min, then kept at 100% B for 3 min, then reset to 85% B. The LC flow rate was 250 μl/min, and 5-μl sample was injected for the liquid chromatography/tandem mass spectrometry analysis. Standards of αGC and

βGC at various concentrations were used to make the external calibration curve used for quantification.

UT Health San Antonio Mass Spectrometry Core Laboratory. Samples were quantified using a standard curve of soluble αGC in isopropanol (2000–125 ng/ml) mixed with 20 μl of a 0.1 mM ceramide-d31 as an internal standard. αGC was extracted from nanoP formulations using 0.1 ml of chloroform/methanol (2:1) plus 20 μl of a 0.1 mM ceramide-d31 internal standard for 200 μl of each nanoP sample. Each sample was vortexed for 10 s, stored at −20°C for 30 min, then 4°C for 30 min, before vortexing and centrifugation (14,000 rpm) at 4°C for 10 min. The chloroform layer (containing αGC) was removed, and chloroform was evaporated by speed vac (Rotovap) for 30 min to dry. To quantify αGC, glycolipid was resuspended in 100 μl of 100% isopropanol, sonicated for 10 min, and centrifuged at 14,000 rpm at 4°C for 10 min before mass spectrometry analysis.

Scanning electron microscopy

Scanning electron microscopy samples were prepared by adding one drop of nanoP solution onto a silicon wafer and dried under vacuum overnight. The dried samples were imaged using a field emission scanning electron microscope JSM-6335 (Tachikawa, Tokyo, Japan). All samples were sputter-coated with 10 Å of palladium (Denton Desk II, Moorestown, NJ) prior to imaging. Images were obtained at a working distance of 15 cm using an acceleration voltage of 10 kV.

In vitro assays

B and T cells were purified by negative selection using pan-B or pan-T MACS bead separation (Miltenyi Biotec) according to the manufacturer's instructions. T and B cell populations were >80% pure. Total splenocytes (2×10^6 cells/ml) or purified B and T cells mixed at 1:1 ratio (1×10^5 cells/ml) were labeled with 0.5 μM CFSE (21888; Sigma-Aldrich) for 9 min in PBS were then quenched with neat FCS and washed extensively before culture. Splenocytes were cultured in a 96-well, flat-bottom tissue culture plate and stimulated with 10 pg/ml or 10 ng/ml of αGC, βGC, nanoP-αGC, nanoP containing βGC (nanoP-βGC), or media only. After 3 d of culture, cells were removed from the wells, labeled with fluorescently tagged lineage specific markers (anti-B220 for B cells and anti-TCRβ plus CD1d-tetramer for iNKT cells) and assessed for cell type–specific CFSE dilution by FACS analysis.

Flow cytometry

Cellular analysis was performed on single-cell suspension of splenocytes treated with RBC lysis buffer (Life Technologies). Flow cytometric analysis was performed with the following mAbs (from BD Biosciences, BioLegend, eBioscience) after blocking with anti-FcRII/III (2.4G2): anti-CD19 (1D3), anti-TCRβ (H57-597), anti-CD4 (GK1.5), anti-CD45R/B220 (RA3-6B2), and anti–IFN-ɤ (XMG1.2). iNKT cells were identified with tetramers of mouse CD1d-αGC (PBS57; U.S. National Institutes of Health Tetramer Core Facility) conjugated to allophycocyanin or PE. Intracellular IFN-ɤ was detected using the Foxp3/Transcription Factor Staining Set (eBioscience). Samples were acquired on an FACSCanto II (BD) or BDFACS Celesta (BD) and were analyzed with FlowJo software (Tree Star).

ELISAs

C57BL/6 mice were bled via submandibular vein by using 16-gauge needle and serum stored at −20°C or −80°C until use. NP-specific IgG and IgM was detected in serum by polysaccharide-specific ELISA. In short, Easy Wash COSTAR 96-well ELISA plates were coated with 2 mg/well serotype 3 polysaccharide from *S. pneumoniae* (no. 172-X; American Type Culture Collection) overnight and then blocked with PBS/5% BSA for 2 h. ELISA plates were washed with PBS/0.05% Tween, and bound serum Ab was detected by HRP anti-mouse IgG or HRP anti-mouse IgM detecting Ab (no. 1030-05, no. 1020-05; Southern-Biotech). ELISA was developed with 550 nM ABTS (Sigma-Aldrich) in 0.1 M citric acid (pH 4.35) + 0.03% H_2O_2 and read on a SPECTRAmax Plus 384 (Molecular Devices) or Epoch2 (BioTek) at 405 nm. Titer was determined to be the lowest dilution that gave an OD higher than 2–3× background.

Mice and immunizations

C57BL/6 wild-type (WT) female mice were housed and bred at the Trudeau Institute or UT Health San Antonio according to the standards of the respective animal care and use committees. All live animal experimental protocols were approved by the Trudeau Institute Animal Care and Use Committee or The UT Health Animal Care and Use Committee. Mice were immunized i.v., s.c., i.m., or intranasally (i.n.) with washed nanoP containing 25 or 50 ng or 0.5 μg/mouse glycolipid in PBS as noted. Equal volumes of control nanoP with no glycolipid were used for comparison. Preliminary in vivo titration studies determined doses of Prevnar13 (Pfizer) and Pneumovax23 (Merck), which provided optimal and suboptimal protection against lethal systemic *S. pneumoniae* in B6 mice (data not shown). Prevnar13 optimal dose 5 mg/mouse or suboptimal dose 0.5 mg/mouse and Pneumovax23 suboptimal dose 1.5 mg/mouse were administered i.p.

In vivo infections

SpPS3 strain URF918 passage 3 clinical isolated obtained by Dr. Kawakami (University of the Ryukyus, Japan) was stored at −80°C until use. Two hundred microliters of thawed bacteria was streaked on blood agar plate (Tryptic Soy Agar with 5% sheep blood; Remel) and incubated for 8 h in 37°C in a 5% CO_2 incubator before collection, serial dilution, and overnight growth in THY broth. SpPS3 was cultured in THY broth growth media (30 g/l of Todd Hewitt broth [Sigma-Aldrich] plus 5 g/l of Bacto Yeast Extract [BD Biosciences]). Mid-log phase growth was identified using a spectrometer (600 nm; BioTek); bacteria were further diluted to 0.1 OD in THY broth and regrown in a CO_2 incubator at 37°C for 2 h. Bacteria were then collected and washed to deliver target dose of *S. pneumoniae* in 200 μl/mouse PBS. C57BL/6 female mice were infected with 200 ml bacteria in PBS (i.v.) to achieve 1×10^8, 1×10^7, 5×10^6, 3×10^6, 2.5×10^6, and 1×10^6 CFU/mouse in vivo as noted. Colonies of *S. pneumoniae* from 7-log serial dilutions of inoculum grown overnight in CO_2 incubator at 37°C on blood agar plate were counted after 24 h to confirm inoculation dose. Mice were observed twice daily for 12 d for evidence of symptoms. Any mouse exhibiting signs of distress, including hunching, shaking, or moribundity, was immediately sacrificed.

Statistics

GraphPad PRISM5 software was used for nonparametric two-tailed *t* tests for normally distributed datasets as noted.

Results

Glycolipid- and S. pneumoniae polysaccharide–loaded PLGA nanoP synthesized by double-emulsion biochemistry

NanoP were synthesized by double-emulsion biochemistry, and differential centrifugation was used to isolate particles smaller than 300 nm by diverse teams at multiple institutions as described in the *Materials and Methods* and depicted in Supplemental Fig. 1A. Experimental vaccine particles contained both αGC and SpPS from SpPS3 (nanoP-αGC-SpPS), whereas control nanoP consisted of nanoP containing αGC (nanoP-αGC), nanoP containing SpPS (nanoP-SpPS), or nanoP containing PBS (nanoP-PBS). Initial particles were characterized by transmission electron microscopy (data not shown) and scanning electron microscopy to confirm sizing (Supplemental Fig. 1B) and ζ sizing to evaluate stability (data not shown). To ensure standard dosing in vitro and in vivo, αGC loading of each batch of particles was determined by LCMS in comparison with an αGC standard curve, either following lipid extraction by chloroform of whole particles, or following dichloromethane dissolution of particles, described in detail in the *Materials and Methods*. SpPS loading of particles was not possible to assess with available chemical techniques, but saturating quantities were used to synthesize the particles, and SpPS-containing particles were used in equal volume to αGC-containing particles to standardize dosing.

αGC PLGA nanoP activate iNKT and B cells in vitro more efficiently than soluble αGC alone

To assess leukocyte stimulation induced by glycolipid-loaded nanoP, we measured the proliferation of murine PBMCs stimulated by soluble glycolipid compared with PLGA encapsulated glycolipid in vitro. iNKT cells proliferated vigorously in response to soluble αGC at the 10-ng/ml dose but failed to respond to the lower, 10 pg/ml dose (Fig. 1A). In contrast, nanoP-αGC stimulated similar iNKT cell proliferation at both the higher (10 ng/ml) and lower doses (10 pg/ml). This is consistent with the notion that nanoP encapsulation of αGC increases the iNKT proliferative response 1000-fold

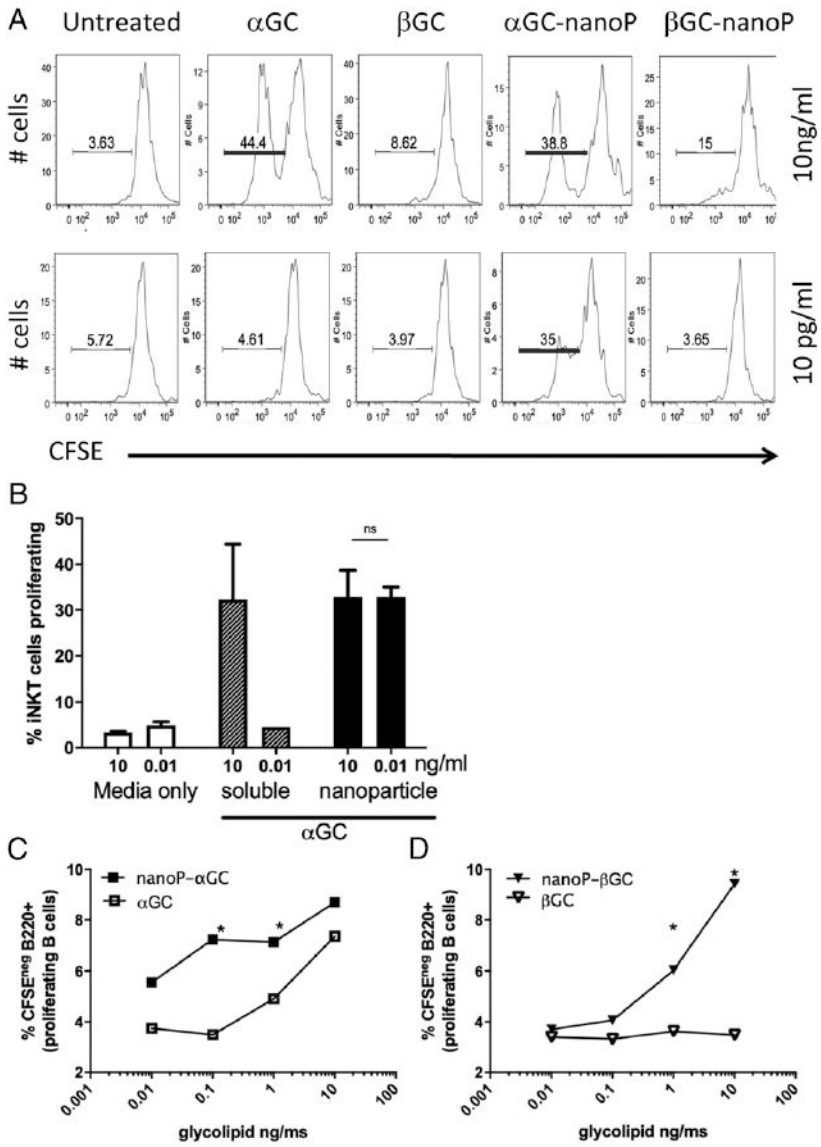

FIGURE 1. Glycolipid adjuvants delivered via nanoP activate iNKT cells and B cells in vitro more efficiently than soluble αGC alone. Spleen cells were isolated from C57BL/6 WT mice then labeled with CFSE and cultured for 3 d with soluble αGC, soluble βGC, nanoP-αGC, or nanoP-βGC at concentrations of glycolipid noted. Flow cytometry histogram gates capture individual examples of frequency of $B220^-$ $TCR\beta^+CD1d\text{-}tet^+$ iNKT cells, which have diluted CFSE as a measure of proliferation (**A**), summarized in bar graph (**B**). The percentages of $B220^+$ $CD19^+$ B cells that dilute CFSE after 3 d of in vitro culture with titrations of soluble αGC or nanoP-αGC as noted (**C**) or soluble βGC and nanoP-βGC (**D**) demonstrate enhanced activity of glycolipids following PLGA encapsulation. Representative of two experiments, duplicate wells. *$p \leq 0.05$ as compared with αGC, by nonparametric Mann–Whitney *t* test (B); two-way ANOVA with Sidak multiple comparison test (C and D).

(summarized in Fig. 1 bar graph). Even the activity of the much less active B-enantiomer form of galactosylceramide, βGC, was modestly enhanced when delivered in the context of nanoP-PBS (Fig. 1A).

To determine if the dose-sparing activity observed by nanoP activation of iNKT cells extended to B cells, we next compared soluble and nanoP delivery of αGC and βGC with B cell in vitro. As observed for iNKT cells, αGC stimulated B cells across a range of doses (10 ng/ml to 10 pg/ml) when delivered in the context of a nanoP, but soluble αGC only stimulated B cells at higher doses (Fig. 1B). The enhancement of B cell activation by nanoP encapsulation can also be observed when using the less active form of glycolipid, βGC. Soluble βGC does not stimulate much B cell proliferation, but nanoP-βGC stimulate a dose-dependent response similar to nanoP-αGC (Fig. 1C). Thus, nanoP-αGC are 1000-fold more efficient at activating both iNKT and B cells than soluble glycolipid alone. This is consistent with dose-sparing effects observed using alternative nanoP formulations from the Irvine laboratory (16).

αGC PLGA nanoP activate iNKT cells in vivo more efficiently than soluble glycolipid

To determine whether nanoP also provided a 1000-fold dose-sparing effect in vivo, we next assessed the in vivo activation of iNKT cells by both soluble and glycolipid-containing nanoP. Both nanoP-αGC and nanoP-βGC stimulated IFN-γ from high frequencies of iNKT cells within 4 h of administration at high doses, but only nanoP-αGC stimulation was sustained at lower doses (Fig. 2A, 2B). Furthermore, as observed in vitro, in vivo administration of nanoP-αGC

also stimulated cytokine production more efficiently than soluble αGC alone (IL-4, Fig. 2C; IFN-γ, Fig. 2D).

In vivo studies next tested whether encapsulation of polysaccharides from *S. pneumoniae* (SpPS) in nanoP containing glycolipid adjuvant (nanoP-αGC) altered the adjuvanticity of the glycolipids. Immunization of WT C57BL/6 mice with nanoP-αGC–induced dose-dependent IFN-γ production by iNKT cells as compared with empty nanoP-PLGA–immunized controls (Fig. 2C). No differences were seen in iNKT cell IFN-γ production between nanoP-αGC and nanoP-αGC-SpPS across the dose ranges (Fig. 2D). This indicates that coencapsulation of *S. pneumoniae* polysaccharides does not inhibit activation efficiency of glycolipid within nanoP-αGC-SpPS. Thus, nanoP that encapsulate the adjuvant αGC-activated iNKT cells more efficiently than soluble αGC in vivo and the efficient in vivo activation of iNKT cells by nanoP-αGC were not impaired by the addition of *S. pneumoniae* polysaccharides.

PLGA nanoP delivery of soluble αGC avoids high-dose iNKT cell anergy

Previous vaccine strategies administered repeated high doses of soluble αGC to enhance immune responses against coadministered Ag, but these approaches induced anergy in iNKT cells (39). Because delivery of αGC via a nanoP platform allows dose sparing of glycolipid, inducing iNKT cell activation with 1000× less nanoP-delivered αGC than is required to elicit equivalent iNKT activation with soluble αGC, we theorized that nanoP administration of αGC would avoid induction of anergy.

To evaluate the potential for nanoP delivery of αGC to avoid anergy, we assessed the capability of iNKT cells to respond to in vitro reactivation following previous in vivo challenge with αGC. First, we immunized B6 WT mice and confirmed iNKT activation by measuring IFN-γ in iNKT cells from the peripheral blood 4 h later (Fig. 3A). We immunized mice with 2 μg αGC, a high dose stimulating significant iNKT cell IFN-γ and expected to induce iNKT cell anergy; 0.5 μg αGC, a submaximal dose which induces significant IFN-γ from iNKT cells, but not as robust as the higher dose; and 0.5 ng nanoP-αGC, which induces significant iNKT IFN-γ at equivalent levels to the soluble 0.5-μg dose (Fig. 3A). To assess anergic status of the iNKT cells following this immunization, we next isolated splenocytes from the mice 7 d after immunization and restimulated the cells in vitro with anti-CD3 and anti-CD28. As expected, iNKT cells from mice immunized with high-dose αGC (2 μg) showed reduced proliferation, reduced IFN-γ, and increased PD-1 expression as compared with the healthy response of naive iNKT cells from control mice pretreated with only PBS (Fig. 3B–D). Thus, the 2 μg–immunized mice exhibit a phenotype consistent with anergy. In contrast, mice activated with a lower dose of αGC (0.5 μg/ms) or nanoP-αGC contained iNKT cells capable of

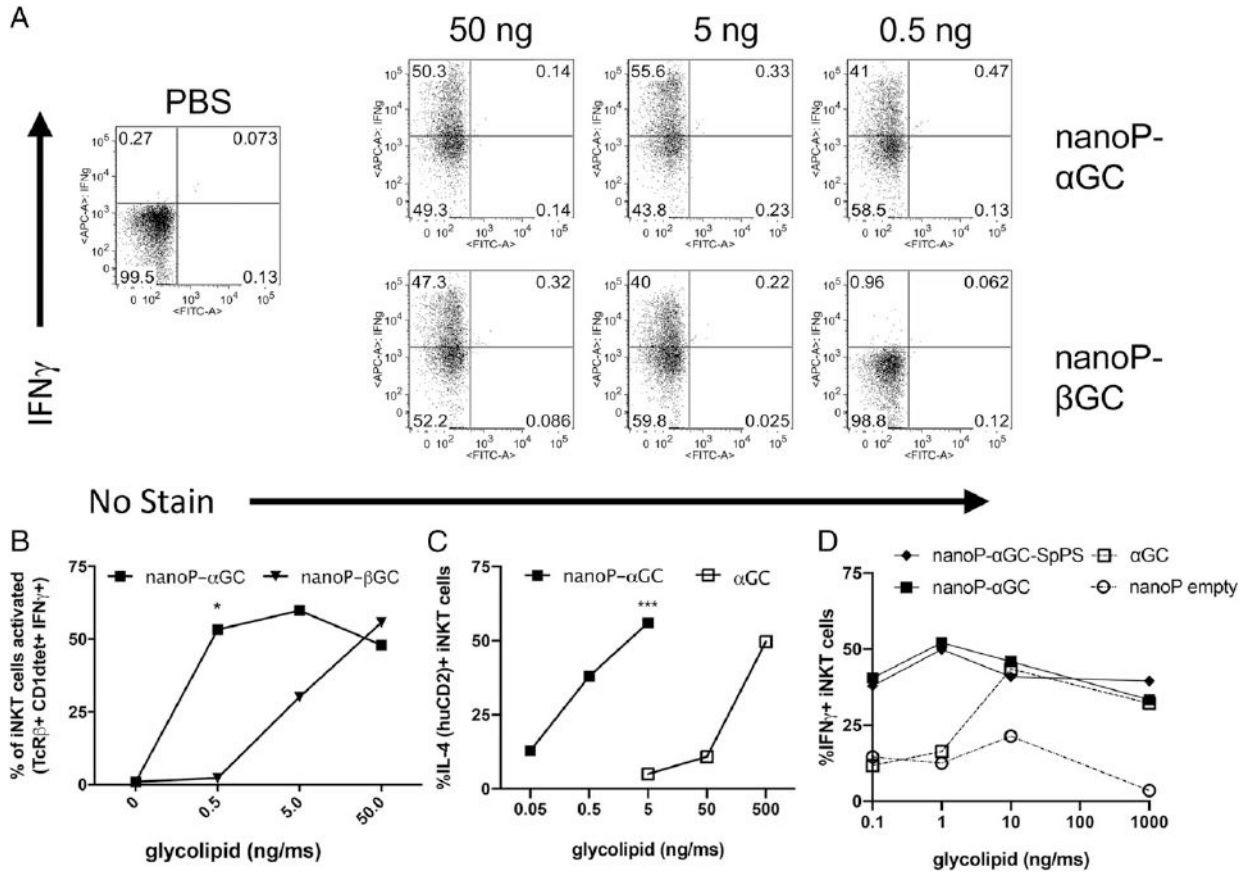

FIGURE 2. Glycolipid adjuvant delivered via PLGA nanoP activates iNKT cells in vivo more efficiently than soluble glycolipid. C57BL/6 WT mice were immunized i.v. with nanoP containing noted concentrations of glycolipid. Percentage of $PLZF^+TCR\beta^+$ iNKT cells that were determined by FACS to be IFN-γ + in spleen 4 h after immunization with various doses of nanoP-αGC or nanoP-βGC (**A**), summarized in (**B**). Percentage of $CD1d\text{-}tet^+$ $TCR\beta^+$ iNKT cells that were determined by FACS to be positive for human CD2, a surrogate reporter for IL-4, per mouse spleen 4 h after immunization with various doses of αGC or nanoP-αGC in vivo (**C**). Immunization with nanoP-αGC and nanoP-αGC-SpPS increased IFN-γ in iNKT cells compared with nanoP-PBS (empty) across a wide dose range in vivo, and both retained activity at doses lower than those for soluble αGC (**D**). $^{***}p < 0.001$, $^{*}p \leq 0.05$, representative of at least two to three experiments, unpaired Welch *t* test (B and C).

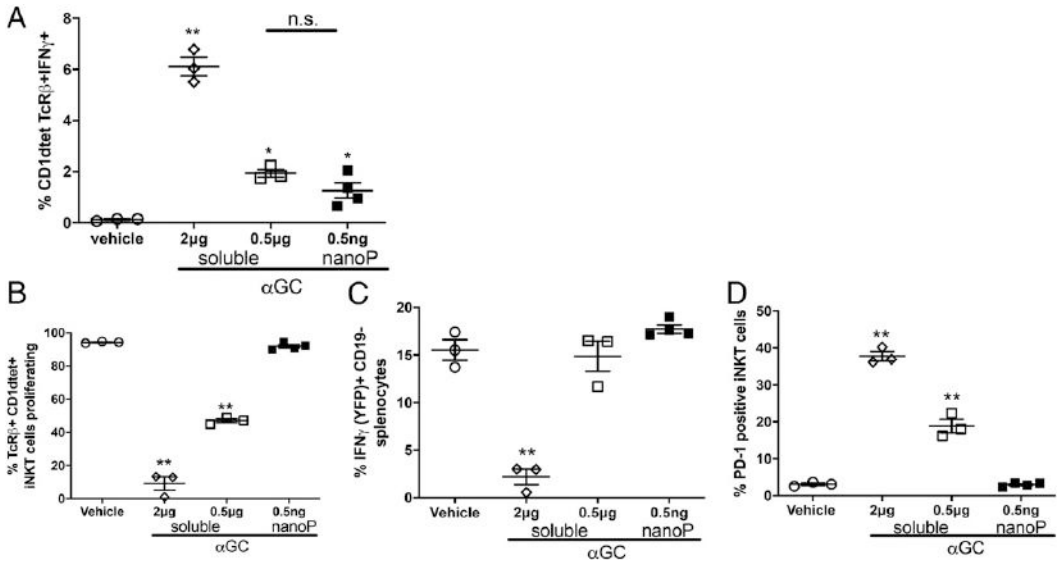

FIGURE 3. PLGA nanoP delivery of soluble αGC avoids high-dose iNKT cell anergy. C57BL/6 WT mice were immunized i.v. with various doses of nanoP-αGC (0.5 ng) or soluble αGC (0.5 and 2 μg). Four hours postimmunization peripheral blood iNKT cell IFN-γ production was measured by flow cytometry (**A**). Seven days after first immunization splenocytes from mice receiving various doses of nanoP-αGC and soluble αGC were isolated and restimulated in vitro with anti-CD3 and anti-CD28. After 24 h, the percentage of $B220^{-}TCR\beta^{+}CD1d\text{-}Tet+$ cells proliferating (**B**), expressing IFN-γ as determined by eYFP reporter signal (**C**), and expressing PD-1 (**D**) was measured by flow cytometry. Frequency comparisons assessed by Welch unpaired *t* test, group mean ± SD, $n = 3$–4 per group. $^{**}p < 0.01$, $^{*}p < 0.05$.

significantly higher levels of proliferation and IFN-γ production (Fig. 3B, 3C) and lower levels of PD-1 (Fig. 3D) than iNKT cells from mice immunized with 2 μg/ms soluble αGC. Instead, low-dose αGC– or nanoP–immunized mice contained iNKT cells responding to restimulation similarly to iNKT cells from previously unimmunized, naive mice (Fig. 3B–D). Thus, nanoP delivery of αGC induces significant iNKT cell activation but avoids an anergic state induced by high-dose soluble αGC administration.

I.v., s.c., and i.m. vaccination with nanoP-αGC-SpPS induces comparable SpPS3-specific IgM and IgG Ab titers

Given that glycolipid-loaded nanoP significantly activate iNKT cells in vivo without inducing anergy, we next evaluated the potential for nanoP-αGC to serve as a vaccine platform. To test the ability of nanoP-delivered glycolipids to enhance an immune response against codelivered pathogen epitopes, polysaccharides from *S. pneumoniae* were coencapsulated with αGC in PLGA nanoP. Prevnar13, an effective peptide-conjugate vaccine currently in use in the clinic, has already demonstrated the importance of *S. pneumoniae* polysaccharide–specific Abs in mediating effective protection against reinfection, so these studies will consider the advantages of nanoP delivery of the well-established protective epitopes in *S. pneumoniae* polysaccharide in combination with a glycolipid adjuvant. To test the idea that αGC can recruit help for polysaccharide-specific protective Ab responses, PLGA nanoP were simultaneously loaded with αGC and SpPS3 and assessed for size, glycolipid loading, and charge (Supplemental Fig. 1) before immunizing C57BL/6J mice. Mice were immunized with soluble SpPS3, coencapsulated nanoP-αGC-SpPS, or control nanoP-PBS on day 0 and boosted on day 31 with serum collected weekly for 7 wk. As expected, mice immunized with nanoP-αGC-SpPS produced robust SpPS3-specific IgM (Fig. 4A) and IgG (Fig. 4B) titers compared with controls immunized with soluble SpPS3 or PLGA nanoP. Importantly, SpPS3-specific IgG Abs were also still detectable on day 70 (Fig. 4B), indicative of a long-term response. Thus, delivery of αGC and SpPS3 simultaneously in a nanoP formulation can induce B cell activation to generate a high-titer Ag-specific IgM and IgG response that is maintained long term.

Initial studies delivered nanoP i.v., but next, we wanted to compare the Ab response generated by nanoP-αGC-SpPS delivered via alternate routes that might be more amenable to human vaccine delivery. As controls, C57BL/6 mice were vaccinated with nanoP-αGC-SpPS (i.v.), nanoP-αGC (i.v.), nanoP-SpPS (i.v.), or Prevnar13 (contains alum, i.p.). As expected, i.v. immunization with nanoP-αGC-SpPS induced significantly higher levels of SpPS3-specific IgM and IgG than nanoP-αGC or nanoP-SpPS alone, with nanoP-αGC-SpPS inducing IgM levels similar to the Prevnar13 vaccine (Fig. 5A, 5B). Thus, i.v. delivery of nanoP-αGC-SpPS generates a high-titer IgM and IgG SpPS3-specific Ab response. Immunization with Prevnar13 is included as a positive control for induction of IgG anti-SpPS titers specific for *S. pneumoniae*. Although the Prevnar13 IgG titer is statistically greater ($p \leq 0.05$) than the response to nanoP-αGC-SpPS (administered i.v.) in Fig. 5B, this is only a measure of Ab titers, not an analysis of Ab affinity or protection/survival, so it is not a true comparison of the effectiveness of the two vaccine strategies. We next tested nanoP-αGC-SpPS vaccines administered s.c., i.m., and i.n. C57BL/6 mice were administered vaccine doses on day 0, and Ab responses were measured weekly by ELISA. Notably, s.c., i.m., and i.v. vaccination routes induced statistically comparable IgG and IgM responses that are significantly different from nanoP-PBS, whereas i.n. delivery was statistically indistinguishable from PBS control (Fig. 5C, 5D). IgM and IgG titers were initially higher following i.v. administration compared with the other routes, but this difference did not persist past day 21, and ultimately, the titers between the i.v., s.c., and i.m. groups were not significantly different. In conclusion, nanoP-αGC-SpPS vaccination induces similar anti-SpPS3 IgG and IgM Ab responses when delivered by multiple routes, establishing the viability of this vaccine approach for human patients.

NanoP-αGC-SpPS protect WT mice from lethal systemic S. pneumoniae infection

Ultimately, the goal of this nanoP formulation is to harness iNKT cell help for Ag-specific B cells to provide long-term protection

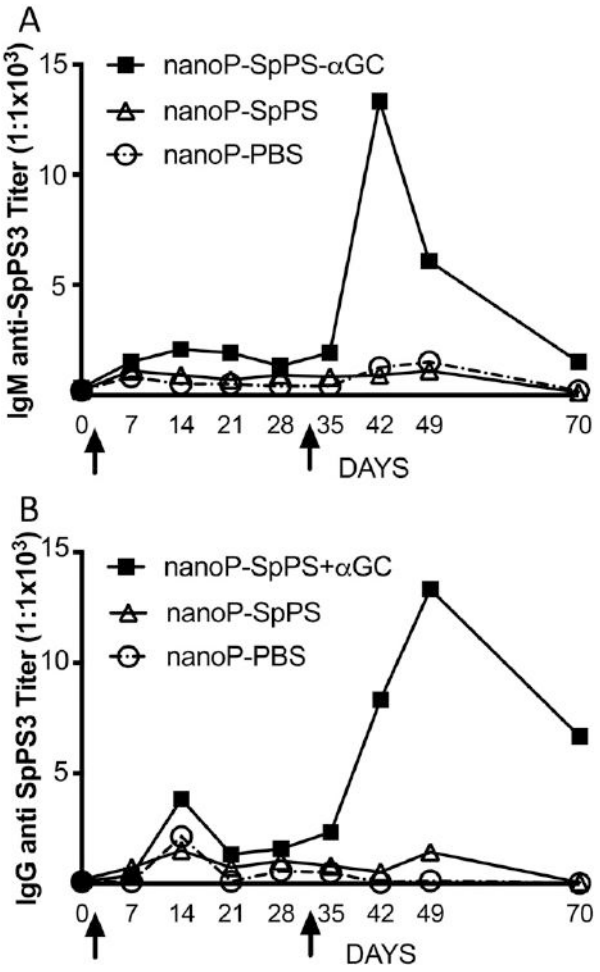

FIGURE 4. In vivo vaccination with glycolipid and SpPS3 nanoP (nanoP-αGC-SpPS) induces SpPS3-specific IgM and IgG Abs. C57BL/6 WT mice were immunized i.v. with PLGA nanoP containing 50 ng glycolipid plus SpPS (nanoP-αGC-SpPS), SpPS alone (nanoP-SpPS), or equivalent volume for PLGA only controls. SpPS-specific IgM (**A**) and IgG (**B**) was detected by ELISA. $n = 4$–6 representative of two experiments.

against reinfection with an important human pathogen. To assess the ability of glycolipid-containing, B cell Ag-embedded nanoP to induce a protective humoral response, we immunized C57BL/6 WT mice with nanoP-αGC-SpPS or control nanoP at days 0 and 30, followed by systemic infection with a lethal dose of *S. pneumoniae* (1.6×10^6). As expected, mice vaccinated with Prevnar13 prior to infection were well protected, and 80% survived a lethal dose of *S. pneumoniae* (Fig. 6A), compared with poor survival (15–30%) in the negative controls receiving no vaccination or nanoP containing only αGC or SpPS. In contrast, nanoP-αGC-SpPS protected the vaccinated mice to nearly the same level as the Prevnar13 controls, providing significantly better protection than the negative control particles. In short, nanoP-αGC-SpPS vaccination protected the majority of the mice infected in vivo with lethal systemic *S. pneumoniae*.

We next considered whether vaccination delivery through different routes was equally protective. C57BL/6 mice were vaccinated identically to mice depicted in Fig. 6A to provide age- and sex-matched controls for comparison with experimental groups receiving 5 ng nanoP-αGC-SpPS delivered i.v., s.c., i.m., or i.n. Consistent with Fig. 6A, Prevnar13 and nanoP-αGC-SpPS protected significantly more mice from lethal *S. pneumoniae* infection than PBS, or control nanoP containing αGC or SpPS alone (Fig. 6B). Mice vaccinated s.c. were equally well protected from death compared with mice vaccinated i.v., whereas mice vaccinated i.m. showed modest protection (Fig. 6C). In contrast, mice vaccinated through the i.n. route were unprotected, and most succumbed to infection. The relative survival of these mice correlated with levels of IgM and IgG SpPS-specific Ab titer detected in each group after immunization (Fig. 5), consistent with the notion that SpPS-specific Abs convey protection. In summary, i.v. and s.c. vaccination induce the most effective protection, with i.m. inducing modest protection and i.n. inducing poor protection.

NanoP-αGC inhibits T-independent, but not T-dependent, humoral vaccine responses

Given the adjuvant effect of coadministering αGC and SpPS by nanoP, we next wanted to determine whether this enhancement effect could extend to coadministration of αGC nanoP and current human vaccines in use in the clinic. To assess an adjuvant effect of nanoP-αGC, we administered particles in combination with either Prevnar13, a T-dependent, peptide-conjugate vaccine with alum adjuvant, or Pneumovax23, a T-independent polysaccharide vaccine. We administered a submaximal dose of Prevnar13 (i.p.) plus 50 ng nanoP-αGC (i.v.) on day 0 and day 30. Prevnar13 induced a modest SpPS-specific IgM and IgG response after the primary immunization and a rigorous memory response after the boost, which was significantly higher than mice treated with nanoP-αGC alone or PBS (Fig. 7A, 7B). Unfortunately, there was no additive increase in SpPS-specific IgM or IgG after vaccinating with a combination of nanoP-αGC and Prevnar13 (Fig. 7A, 7B), suggesting iNKT cell help does not enhance a B cell response that is already receiving optimal $CD4^+$ T cell help. Following both vaccinations, mice were infected with a systemic lethal dose of *S. pneumoniae* and monitored for survival. Survival of treated groups reflected the Ab titers, both Prevnar13- and nanoP-αGC plus Prevnar13–treated groups were significantly protected as compared with nanoP-αGC– or PBS-treated controls (Fig. 7C).

Next, we vaccinated mice with both nanoP-αGC and the T-independent vaccine, Pneumovax23, to see if activation of iNKT cells by nanoP-αGC could enhance the activity of a vaccine that does not normally recruit T cell help. Pneumovax23 induced a modest SpPS-specific IgM titer, which was really only evident after the second boost (Fig. 7D). Pneumovax23 induced a significant IgG anti-SpPS titer, which increased dramatically after a boost (Fig. 7E). To our surprise, coadministering nanoP-αGC with Pneumovax23 led to a reduction in SpPS-specific IgG as compared with the titers induced with Pneumovax23 alone. Both Pneumovax23 and Pneumovax23 plus nanoP-αGC were higher than unvaccinated mice during the primary response, but after the second boost, the Ag-specific titer in the nanoP-αGC–cotreated mice was reduced to levels equivalent to the unvaccinated mice (Fig. 7E). These data suggest that administration of nanoP-αGC with a soluble T-independent Ag may induce negative regulation of B cells by iNKT cells. Following both vaccinations, mice were all infected with a systemic lethal dose of *S. pneumoniae* and monitored for survival. Survival reflected the SpPS-specific Ab titers, and mice vaccinated with Pneumovax23 were protected from death as compared with mice vaccinated with only nanoP-αGC or PBS. The protection provided by Pneumovax23 was reduced when mice were cotreated with soluble αGC, or to a lesser extent, nanoP-αGC (Fig. 7F). Future studies are needed to dissect this unexpected inhibitory effect.

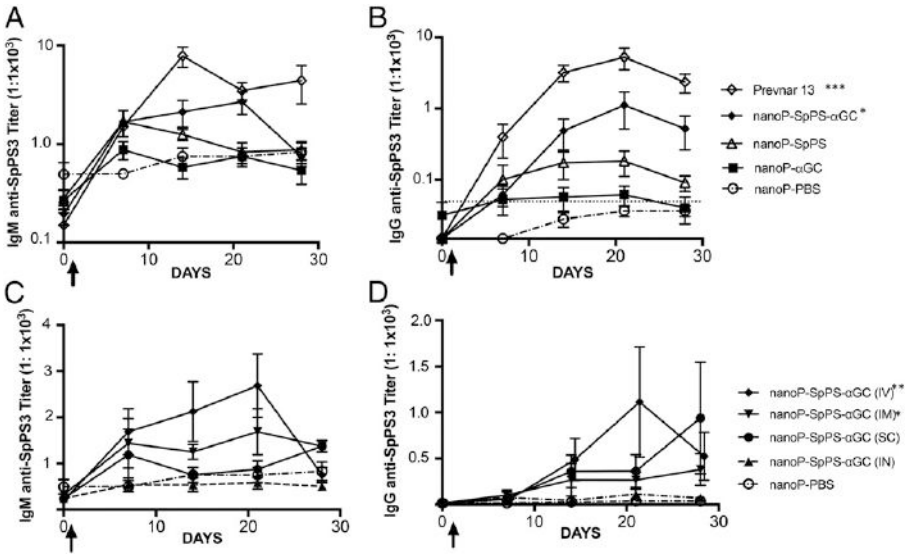

FIGURE 5. NanoP-SpPS-αGC stimulate IgG anti-SpPS when administered i.v., s.c., or i.m., but not i.n. C57BL/6 WT mice were immunized with nanoP containing 50 ng/mouse αGC or equal volumes of control nanoP, as labeled: nanoP-αGC, nanoP-SpPS, nanoP-SpPS-αGC, Prevnar13, or PBS before weekly bleeds to assess SpPS3-specific IgM titers (**A**) or SpPS3-specific IgG titers (**B**) by ELISA. In comparison with nanoP-SpPS-αGC administered i.v. in (A) and (B), they were also delivered via alternative routes: i.m., s.c., and i.n. and followed via weekly bleeds and ELISA for SpPS3-specific IgM (**C**) and IgG (**D**). Representative of two experiments. $n = 5$ mice per group; two-way ANOVA. ***$p \leq 0.001$, **$p \leq 0.01$, *$p \leq 0.05$ as compared with nanoP-PBS group for both IgM and IgG.

Discussion

These studies examine the potential for an iNKT-activating glycolipid-loaded nanoP vaccine to provide supporting signals to B cells to generate protective Abs against systemic lethal infection by *S. pneumoniae*. *S. pneumoniae* polysaccharide was selected as the B cell epitope to be combined with αGC adjuvant in this vaccine because it induces protective Ab responses in vaccines currently in use in the clinic: Prevnar13 and Pneumovax23. Prevnar13 is an effective pneumococcal vaccine that induces a T cell dependent immune response. However, the protection level of this vaccine varies from one individual to another because it depends on diverse MHC class II–restricted $CD4^+$ T cell recognition. αGC-loaded nanoP vaccines avoid this challenge by activating iNKT cells that bind glycolipid Ags presented by the nonpolymorphic Ag-presenting molecule CD1d, reducing allelic variability in the immune response. *S. pneumoniae* has many serotypes that cause serious pneumococcal infection but are not covered by current clinical vaccines, so even though this pathogen was selected as a target for testing αGC delivery by nanoP as a platform, this approach could also fill the need for a new *S. pneumoniae* vaccine capable of inducing protection against multiple serotypes. Synthesis of glycolipid and polysaccharide embedded nanoP lends itself to combining polysaccharides from multiple different serotypes of *S. pneumoniae* in one nanoP formulation. Although the nanoP vaccine approach evaluated in this study will potentially provide a new alternative, to our knowledge, for protection against *S. pneumoniae*, it should also serve as a proof of principle underpinning the future development of related vaccines for other encapsulated pathogens.

NanoP synthesized by an optimized double-emulsion protocol were routinely tested for size and charge by scanning electron microscopy or Zetasizer and αGC loading by LCMS to standardize dosing. Technical challenges prevented loading assessment of polysaccharides, so a saturating amount of SpPS3 was included during the synthesis process to ensure that nanoP were sufficiently loaded with SpPS3. Induction of both iNKT cell activation and SpPS3-specific Ab responses were confirmed in vivo for each nanoP batch before use. Initial testing confirmed that αGC-containing nanoP induced in vitro proliferation and in vitro and in vivo cytokine production by iNKT cells. Importantly, these studies showed that nanoP containing αGC activate iNKT cells at doses 1000× lower than we or others routinely use for in vivo studies with soluble glycolipids [0.5 μg/mouse (40) or 2 μg/mouse (41)]. This dose-sparing effect has been documented by other nanoP formulations (16) and minimizes off target effects, enables efficient iNKT and B cell activation, and provides for the cost savings inherent in reduced Ag use. We also discovered that dose sparing enabled by efficient nanoP delivery of αGC provided an additional advantage in that this nanoP delivery mechanism avoided iNKT cell anergy induced by repeated exposure to high doses of αGC. Avoiding anergy is a critical requirement for any vaccine administered in multiple or repeated doses, and this benefit highlights the potential for αGC to be used for future vaccine development.

We next confirmed that nanoP-αGC-SpPS stimulate B cell proliferation in vitro and drive production of significant SpPS-specific IgM and IgG Ab titers in vivo. Interestingly, nanoP-αGC-SpPS drives higher secondary titers of both IgM and IgG anti-SpPS–specific Abs following a boost, consistent with development of both IgM and IgG memory B cells. IgM memory B cells contribute an important defense against recurrent pneumococcal infection (32), and IgM Abs are crucial for opsonization against pneumococcal polysaccharide Ags (33), so both IgM and IgG are important in maintaining protection against *S. pneumoniae*. The administration of soluble αGC, haptenated αGC, and particulate αGC + protein have been previously shown to expand $iNKT_{FH}$ cells in vivo (37), so the possibility that $iNKT_{FH}$ cells may specifically enhance germinal center development of polysaccharide-specific IgM^+ memory B cells is intriguing but remains to be confirmed. Furthermore, previous studies from our own laboratory and others have found that $iNKT_{FH}$ cells can be expanded in the absence of humoral memory against certain Ags (37, 40), whereas others have described polysaccharide-specific humoral memory in the apparent absence of $iNKT_{FH}$ cells

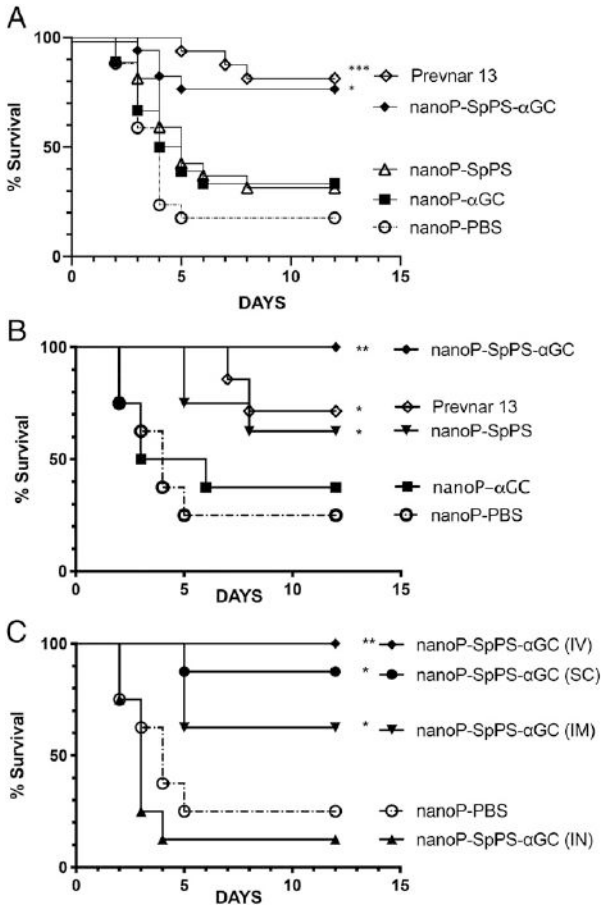

FIGURE 6. NanoP-SpPS-αGC protects mice from lethal systemic *S. pneumoniae*. i.v. nanoP-αGC-SpPS (50 ng/mouse) protects WT B6 mice from systemic, lethal *S. pneumoniae* better than controls, nanoP-SpPS, nanoP-αGC, and nanoP-PBS and at similar level to 0.5 μg Prevnar13. (**A**) In a subsequent experiment, controls revealed similar outcomes (**B**), whereas 50 ng/mouse nanoP-SpPS-αGC provided similar protection by i.v. and s.c. routes, modest protection by i.m. route, and poor protection by i.n. route (**C**). Pool of two experiments, 1.6×10^6 CFU/mouse. $n = 5$–10 per group (grp). (A) Representative of two experiments, 1.6×10^6 CFU/mouse. $n = 5$–8 per grp. (B and C) ***$p \leq 0.001$, **$p \leq 0.01$, *$p \leq 0.05$ as compared with nanoP-PBS.

(15), so whether $iNKT_{FH}$ cells are necessary or sufficient for humoral memory remains an open question.

To identify the nanoP vaccine delivery route that stimulates maximal IgM and IgG Ab production, four different routes of vaccine administration were compared. We found that i.v., i.m., and s.c. routes induced titers of SpPS3-specific IgM and IgG comparable to those induced by Prevnar13. Within the first few weeks, titers were variable, and the i.v. route did appear to induce higher initial IgM and IgG titers, but the long-term Ab titer after 30 d was similar for all three routes. Most importantly, vaccines administered by all three routes enhanced mouse survival after pneumococcal systemic lethal infection at equivalent rates. In contrast, i.n. delivery of vaccine did not stimulate IgM or IgG anti-SpPS3 above preinjection levels and did not enhance mouse survival rate after pneumococcal systemic lethal infection. Abs induced by i.n. vaccine administration are more likely to be IgA and might be limited to the pulmonary compartment, where they could potentially protect better against pneumoniae than sepsis. This remains to be tested but suggests i.n. may be a less relevant route of vaccination for systemic infection.

Given the effectiveness of nanoP encapsulated αGC as an adjuvant for coencapsulated pathogen Ags, we next assessed whether this same enhancement effect could apply to other coadministered vaccines. To test this possibility, we coadministered αGC-nanoP with suboptimal doses of Prevnar13 and Pneumovax23, the two *S. pneumoniae* vaccines currently in use in the clinic for human patients. These two vaccines both induce protective Ab responses against *S. pneumoniae* but through different B cell mechanisms. Prevnar13 is comprised of polysaccharides from 13 serotypes conjugated to an antigenic peptide, which recruits T cell help for the B cell polysaccharide-specific response and induces a high-titer, class-switched, protective Ab response (42). Alternatively, Pneumovax23 is comprised of a mixture of polysaccharides from 23 different serotypes, induces a more modest T-independent response, recruits no T cell help (42), and is also protective against infection, but to a slightly lesser degree than Prevnar13. We expected that coadministering nanoP-αGC with one of these other vaccines would recruit iNKT cell help to enhance IgM and IgG titers induced by both Prevnar13 and Pneumovax23. Coadministering nanoP-αGC or soluble αGC in combination with a suboptimal dose of Prevnar13 induced similar IgM and IgG anti-SpPS3–specific Abs as Prevnar13 alone. Coadministration of αGC could not enhance survival because Prevnar13 fully protected 100% of the mice, but not all mice survived when both nanoP-αGC and Prevnar13 were administered together, further suggesting this combination did not enhance the Prevnar13 response.

Next, we considered the effect of coadministering nanoP-αGC with the other *S. pneumoniae* vaccine (Pneumovax23) used in the clinic. Surprisingly, we found that coadministration of nanoP-αGC or soluble αGC with a suboptimal dose of Pneumovax23 did not significantly improve Pneumovax23-induced IgM SpPS3-specific Abs and actually reduced the titers of primary and secondary anti-SpPS3 IgG specific Abs. Furthermore, the coadministration of nanoP-αGC with a suboptimal dose of Pneumovax23 provided significantly poorer protection against systemic lethal *S. pneumoniae* infection than Pneumovax23 alone. This is a very surprising effect, which is consistent with the possibility that B cells exposed to αGC and soluble polysaccharide become tolerized, undergo apoptosis, and/or are killed, potentially by regulatory iNKT cells. Pneumovax vaccination may create an environment similar to the chronic inflammation induced by pathogen- or damage-associated molecular patterns from a pathogen or autoimmune-mediated inflammation. Our previous studies found that chronic inflammation induces a regulatory iNKT cell phenotype that licenses iNKT cells to eliminate Ag-specific B cells (38). We have previously examined the activity of iNKT cells when acutely activated by αGC in the context of chronic stimulation and found that this combination avoids the iNKT killer phenotype and instead expands $iNKT_{FH}$ cells to actively support an ongoing B cell response (36). However, coadministration of nanoP-SpPS-αGC reduces the in vivo Ab response to Pneumovax23, which is inconsistent with an expansion of $iNKT_{FH}$ cell function. Instead, these data are more consistent with evidence that repeated administration of soluble polysaccharides plus adjuvant leads to transient B cell hyporesponsiveness, which is thought to be mediated by memory B cell apoptosis (43). Importantly, a contribution of iNKT cells to polysaccharide-induced memory B cell hyporesponsiveness has not yet been considered. So, in short, coadministration of Pneumovax and nanoP-SpPS-αGC is likely to create a complicated interplay of differences in both iNKT cell and B cells, which we intend to dissect in future studies.

In summary, these studies reveal the advantages of using a nanoP formulation to coencapsulate a glycolipid adjuvant, αGC, and B cell

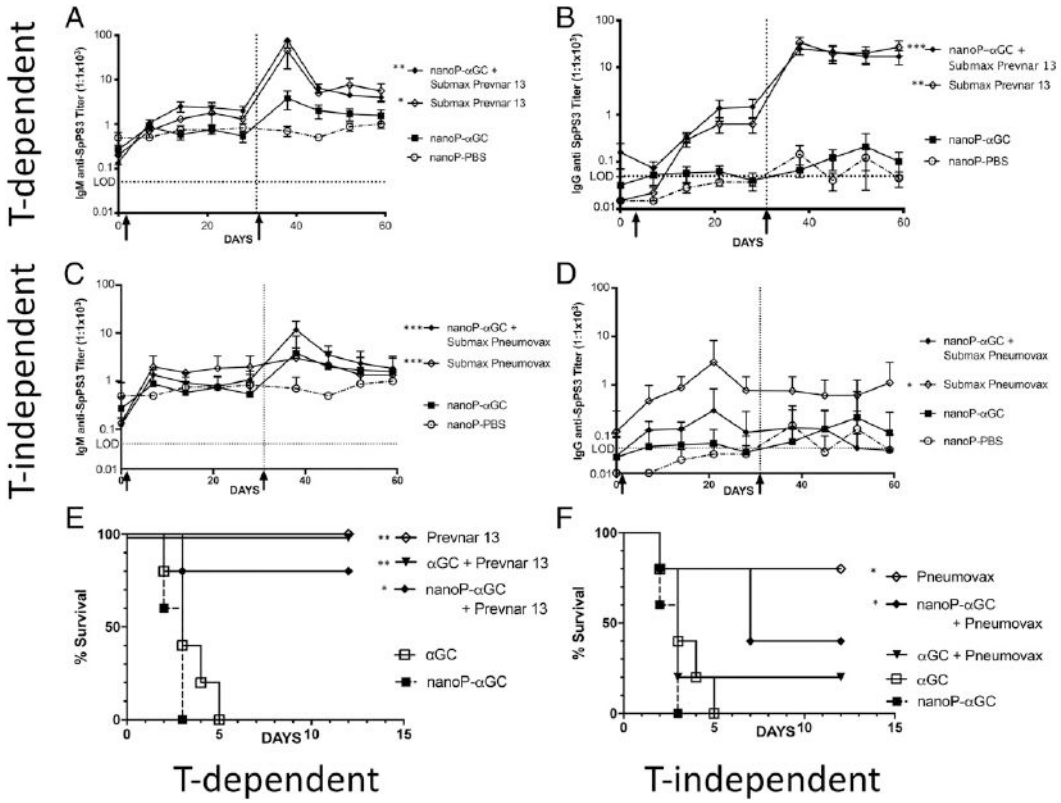

FIGURE 7. NanoP-αGC inhibit T-independent, but not T-dependent, humoral vaccine responses. ELISA revealed serum titers of SpPS3-specific IgM and IgG following coadministration of nanoP-αGC (i.v., 50 μg/ms) or soluble αGC (0.5 ng/ms) plus submaximal protective doses of i.p. Prevnar13 (0.5 μg/ms) [IgM (**A**) and IgG (**B**)] or i.p. Pneumovax23 (1.5 μg/ms) [IgM (**C**) and IgG (**D**)] or controls, nanoP-αGC (50 μg/ms), and nanoP-PBS (200 μl). Primary immunizations were on day 0, boost with half the nanoP dose (25 ng/mouse for nanoP groups [grp]) on day 31. The same mice were then infected with systemic *S. pneumoniae* (1.6×10^6 CFU/ms, i.v.) on day 60 and observed for 12 d postinfection (**E** and **F**). Representative of two experiments, $n = 6$–8 mice per grp; two-way ANOVA. $^{***}p < 0.001$, $^{**}p < 0.01$, $^{*}p < 0.05$ compared with nanoP-PBS (A–D) or nanoP-αGC (E and F).

protective epitope, SpPS3, for formulating a protective new vaccine strategy. NanoP delivery of αGC stimulates high-titer, protective IgG and IgM memory responses against systemic lethal *S. pneumoniae*. However, coadministration of αGC, soluble or via nanoP, with soluble polysaccharides significantly reduces polysaccharide-specific B cell responses, suggesting iNKT cells could also tolerize or eliminate Ag-specific B cells under certain delivery conditions. This dichotomy has important implications for the regulatory mechanisms at play between iNKT cells and B cells during acute or chronic inflammation and merits further investigation.

Acknowledgments

We thank the National Institutes of Health Tetramer Core Facility, Emory University, for providing mCD1d-PBS57 tetramer for our flow cytometry studies.

Disclosures

E.A., A.W., E.V.-D., J.M., R.J.L., and E.A.L. are inventors on patent 10,881,720, issued January 5, 2021, "Nanoparticles for Immune Stimulation." The other authors have no financial conflicts of interest.

References

1. Leadbetter, E. A., and M. C. I. Karlsson. 2021. Reading the room: iNKT cells influence B cell responses. *Mol. Immunol.* 130: 49–54.
2. Dellabona, P., S. Abrignani, and G. Casorati. 2014. iNKT-cell help to B cells: a cooperative job between innate and adaptive immune responses. *Eur. J. Immunol.* 44: 2230–2237.
3. Galli, G., P. Pittoni, E. Tonti, C. Malzone, Y. Uematsu, M. Tortoli, D. Maione, G. Volpini, O. Finco, S. Nuti, et al. 2007. Invariant NKT cells sustain specific B cell responses and memory. *Proc. Natl. Acad. Sci. USA* 104: 3984–3989.
4. Galli, G., S. Nuti, S. Tavarini, L. Galli-Stampino, C. De Lalla, G. Casorati, P. Dellabona, and S. Abrignani. 2003. CD1d-restricted help to B cells by human invariant natural killer T lymphocytes. *J. Exp. Med.* 197: 1051–1057.
5. Leadbetter, E. A., M. Brigl, P. Illarionov, N. Cohen, M. C. Luteran, S. Pillai, G. S. Besra, and M. B. Brenner. 2008. NK T cells provide lipid antigen-specific cognate help for B cells. *Proc. Natl. Acad. Sci. USA* 105: 8339–8344.
6. Fujii, S., K. Shimizu, M. Kronenberg, and R. M. Steinman. 2002. Prolonged IFN-gamma-producing NKT response induced with alpha-galactosylceramide-loaded DCs. *Nat. Immunol.* 3: 867–874.
7. Matsuda, J. L., L. Gapin, J. L. Baron, S. Sidobre, D. B. Stetson, M. Mohrs, R. M. Locksley, and M. Kronenberg. 2003. Mouse V alpha 14i natural killer T cells are resistant to cytokine polarization in vivo. *Proc. Natl. Acad. Sci. USA* 100: 8395–8400.
8. Parekh, V. V., M. T. Wilson, D. Olivares-Villagómez, A. K. Singh, L. Wu, C. R. Wang, S. Joyce, and L. Van Kaer. 2005. Glycolipid antigen induces long-term natural killer T cell anergy in mice. *J. Clin. Invest.* 115: 2572–2583.
9. Singh, N., S. Hong, D. C. Scherer, I. Serizawa, N. Burdin, M. Kronenberg, Y. Koezuka, and L. Van Kaer. 1999. Cutting edge: activation of NK T cells by CD1d and alpha-galactosylceramide directs conventional T cells to the acquisition of a Th2 phenotype. *J. Immunol.* 163: 2373–2377.
10. Treuel, L., X. Jiang, and G. U. Nienhaus. 2013. New views on cellular uptake and trafficking of manufactured nanoP. *J. R. Soc. Interface* 10: 20120939.
11. Chang, T. Z., S. S. Stadmiller, E. Staskevicius, and J. A. Champion. 2017. Effects of ovalbumin protein nanoP vaccine size and coating on dendritic cell processing. *Biomater. Sci.* 5: 223–233.
12. Kaminskas, L. M., and C. J. Porter. 2011. Targeting the lymphatics using dendritic polymers (dendrimers). *Adv. Drug Deliv. Rev.* 63: 890–900.
13. Manolova, V., A. Flace, M. Bauer, K. Schwarz, P. Saudan, and M. F. Bachmann. 2008. NanoPs target distinct dendritic cell populations according to their size. *Eur. J. Immunol.* 38: 1404–1413.
14. Thapa, P., G. Zhang, C. Xia, A. Gelbard, W. W. Overwijk, C. Liu, P. Hwu, D. Z. Chang, A. Courtney, J. K. Sastry, et al. 2009. NanoP formulated alpha-galactosylceramide activates NKT cells without inducing anergy. *Vaccine* 27: 3484–3488.

15. Bai, L., S. Deng, R. Reboulet, R. Mathew, L. Teyton, P. B. Savage, and A. Bendelac. 2013. Natural killer T (NKT)-B-cell interactions promote prolonged antibody responses and long-term memory to pneumococcal capsular polysaccharides. *Proc. Natl. Acad. Sci. USA* 110: 16097–16102.
16. Bershteyn, A., M. C. Hanson, M. P. Crespo, J. J. Moon, A. V. Li, H. Suh, and D. J. Irvine. 2012. Robust IgG responses to nanograms of antigen using a biomimetic lipid-coated particle vaccine. *J. Control. Release* 157: 354–365.
17. Macho-Fernandez, E., L. J. Cruz, R. Ghinnagow, J. Fontaine, E. Bialecki, B. Frisch, F. Trottein, and C. Faveeuw. 2014. Targeted delivery of α-galactosylceramide to CD8α+ dendritic cells optimizes type I NKT cell-based antitumor responses. *J. Immunol.* 193: 961–969.
18. Courtney, A. N., P. Thapa, S. Singh, A. M. Wishahy, D. Zhou, and J. Sastry. 2011. Intranasal but not intravenous delivery of the adjuvant α-galactosylceramide permits repeated stimulation of natural killer T cells in the lung. *Eur. J. Immunol.* 41: 3312–3322.
19. Danhier, F., E. Ansorena, J. M. Silva, R. Coco, A. Le Breton, and V. Préat. 2012. PLGA-based nanoP: an overview of biomedical applications. *J. Control. Release* 161: 505–522.
20. O'Hagan, D. T., D. Rahman, J. P. McGee, H. Jeffery, M. C. Davies, P. Williams, S. S. Davis, and S. J. Challacombe. 1991. Biodegradable microparticles as controlled release antigen delivery systems. *Immunology* 73: 239–242.
21. Danhier, F., O. Feron, and V. Préat. 2010. To exploit the tumor microenvironment: passive and active tumor targeting of nanocarriers for anti-cancer drug delivery. *J. Control. Release* 148: 135–146.
22. Tahara, K., T. Sakai, H. Yamamoto, H. Takeuchi, N. Hirashima, and Y. Kawashima. 2009. Improved cellular uptake of chitosan-modified PLGA nanospheres by A549 cells. *Int. J. Pharm.* 382: 198–204.
23. Prokop, A., and J. M. Davidson. 2008. Nanovehicular intracellular delivery systems. *J. Pharm. Sci.* 97: 3518–3590.
24. Park, Y. S. 2002. Tumor-directed targeting of liposomes. *Biosci. Rep.* 22: 267–281.
25. Ishida, T., K. Atobe, X. Wang, and H. Kiwada. 2006. Accelerated blood clearance of PEGylated liposomes upon repeated injections: effect of doxorubicin-encapsulation and high-dose first injection. *J. Control. Release* 115: 251–258.
26. Ishida, T., M. Ichihara, X. Wang, and H. Kiwada. 2006. Spleen plays an important role in the induction of accelerated blood clearance of PEGylated liposomes. *J. Control. Release* 115: 243–250.
27. Ishida, T., M. Ichihara, X. Wang, K. Yamamoto, J. Kimura, E. Majima, and H. Kiwada. 2006. Injection of PEGylated liposomes in rats elicits PEG-specific IgM, which is responsible for rapid elimination of a second dose of PEGylated liposomes. *J. Control. Release* 112: 15–25.
28. Ahmed, S. S., T. Pondo, W. Xing, L. McGee, M. Farley, W. Schaffner, A. Thomas, A. Reingold, L. H. Harrison, R. Lynfield, et al. 2020. Early impact of 13-valent pneumococcal conjugate vaccine use on invasive pneumococcal disease among adults with and without underlying medical conditions-United States. *Clin. Infect. Dis.* 70: 2484–2492.
29. Slotved, H. C., T. Dalby, and S. Hoffmann. 2016. The effect of pneumococcal conjugate vaccines on the incidence of invasive pneumococcal disease caused by ten non-vaccine serotypes in Denmark. *Vaccine* 34: 769–774.
30. Feikin, D. R., E. W. Kagucia, J. D. Loo, R. Link-Gelles, M. A. Puhan, T. Cherian, O. S. Levine, C. G. Whitney, K. L. O'Brien, and M. R. Moore; Serotype Replacement Study Group. 2013. Serotype-specific changes in invasive pneumococcal disease after pneumococcal conjugate vaccine introduction: a pooled analysis of multiple surveillance sites. *PLoS Med.* 10: e1001517.
31. Balsells, E., L. Guillot, H. Nair, and M. H. Kyaw. 2017. Serotype distribution of Streptococcus pneumoniae causing invasive disease in children in the post-PCV era: a systematic review and meta-analysis. *PLoS One* 12: e0177113.
32. Kruetzmann, S., M. M. Rosado, H. Weber, U. Germing, O. Tournilhac, H. H. Peter, R. Berner, A. Peters, T. Boehm, A. Plebani, et al. 2003. Human immunoglobulin M memory B cells controlling Streptococcus pneumoniae infections are generated in the spleen. *J. Exp. Med.* 197: 939–945.
33. Cho, H. K., I. H. Park, R. L. Burton, and K. H. Kim. 2016. Impact of IgM antibodies on cross-protection against pneumococcal serogroups 6 and 19 after immunization with 7-valent pneumococcal conjugate vaccine in children. *J. Korean Med. Sci.* 31: 950–956.
34. Musher, D. M., A. J. Chapman, A. Goree, S. Jonsson, D. Briles, and R. E. Baughn. 1986. Natural and vaccine-related immunity to Streptococcus pneumoniae. *J. Infect. Dis.* 154: 245–256.
35. Stein, K. E. 1992. Thymus-independent and thymus-dependent responses to polysaccharide antigens. *J. Infect. Dis.* 165(Suppl. 1): S49–S52.
36. Sedimbi, S. K., T. Hägglöf, M. G. Garimella, S. Wang, A. Duhlin, A. Coelho, K. Ingelshed, E. Mondoc, S. G. Malin, R. Holmdahl, et al. 2020. Combined proinflammatory cytokine and cognate activation of invariant natural killer T cells enhances anti-DNA antibody responses. *Proc. Natl. Acad. Sci. USA* 117: 9054–9063.
37. Vomhof-DeKrey, E. E., J. Yates, T. Hägglöf, P. Lanthier, E. Amiel, N. Veerapen, G. S. Besra, M. C. Karlsson, and E. A. Leadbetter. 2015. Cognate interaction with iNKT cells expands IL-10-producing B regulatory cells. *Proc. Natl. Acad. Sci. USA* 112: 12474–12479.
38. Hägglöf, T., S. K. Sedimbi, J. L. Yates, R. Parsa, B. H. Salas, R. A. Harris, E. A. Leadbetter, and M. C. Karlsson. 2016. Neutrophils license iNKT cells to regulate self-reactive mouse B cell responses. *Nat. Immunol.* 17: 1407–1414.
39. Huang, J. R., Y. C. Tsai, Y. J. Chang, J. C. Wu, J. T. Hung, K. H. Lin, C. H. Wong, and A. L. Yu. 2014. α-Galactosylceramide but not phenyl-glycolipids induced NKT cell anergy and IL-33-mediated myeloid-derived suppressor cell accumulation via upregulation of egr2/3. *J. Immunol.* 192: 1972–1981.
40. King, I. L., A. Fortier, M. Tighe, J. Dibble, G. F. Watts, N. Veerapen, A. M. Haberman, G. S. Besra, M. Mohrs, M. B. Brenner, and E. A. Leadbetter. 2011. Invariant natural killer T cells direct B cell responses to cognate lipid antigen in an IL-21-dependent manner. *Nat. Immunol.* 13: 44–50.
41. Chang, P. P., P. Barral, J. Fitch, A. Pratama, C. S. Ma, A. Kallies, J. J. Hogan, V. Cerundolo, S. G. Tangye, R. Bittman, et al. 2011. Identification of Bcl-6-dependent follicular helper NKT cells that provide cognate help for B cell responses. *Nat. Immunol.* 13: 35–43.
42. Pollard, A. J., K. P. Perrett, and P. C. Beverley. 2009. Maintaining protection against invasive bacteria with protein-polysaccharide conjugate vaccines. *Nat. Rev. Immunol.* 9: 213–220.
43. Brynjolfsson, S. F., M. Henneken, S. P. Bjarnarson, E. Mori, G. Del Giudice, and I. Jonsdottir. 2012. Hyporesponsiveness following booster immunization with bacterial polysaccharides is caused by apoptosis of memory B cells. *J. Infect. Dis.* 205: 422–430.